



# Filtering electrocardiographic signals using an unbiased and normalized adaptive noise reduction system

Yunfeng Wu<sup>a,\*</sup>, Rangaraj M. Rangayyan<sup>b</sup>, Yachao Zhou<sup>c</sup>, Sin-Chun Ng<sup>d</sup>

<sup>a</sup> School of Information Engineering, Beijing University of Posts and Telecommunications, 10 Xi Tu Cheng Road, Haidian District, Beijing 100876, China

<sup>b</sup> Department of Electrical and Computer Engineering, Schulich School of Engineering, University of Calgary, 2500 University Drive N.W., Calgary, AB T2N 1N4, Canada

<sup>c</sup> Department of Computer Science and Technology, Tsinghua University, Beijing 100084, China

<sup>d</sup> School of Science and Technology, Open University of Hong Kong, 30 Good Shepherd Street, Homantin, Kowloon, Hong Kong, China

Received 4 December 2007; received in revised form 25 March 2008; accepted 28 March 2008

## Abstract

We present a novel unbiased and normalized adaptive noise reduction (UNANR) system to suppress random noise in electrocardiographic (ECG) signals. The system contains procedures for the removal of baseline wander with a two-stage moving-average filter, comb filtering of power-line interference with an infinite impulse response (IIR) comb filter, an additive white noise generator to test the system's performance in terms of signal-to-noise ratio (SNR), and the UNANR model that is used to estimate the noise which is subtracted from the contaminated ECG signals. The UNANR model does not contain a bias unit, and the coefficients are adaptively updated by using the steepest-descent algorithm. The corresponding adaptation process is designed to minimize the instantaneous error between the estimated signal power and the desired noise-free signal power. The benchmark MIT-BIH arrhythmia database was used to evaluate the performance of the UNANR system with different levels of input noise. The results of adaptive filtering and a study on convergence of the UNANR learning rate demonstrate that the adaptive noise-reduction system that includes the UNANR model can effectively eliminate random noise in ambulatory ECG recordings, leading to a higher SNR improvement than that with the same system using the popular least-mean-square (LMS) filter. The SNR improvement provided by the proposed UNANR system was higher than that provided by the system with the LMS filter, with the input SNR in the range of 5–20 dB over the 48 ambulatory ECG recordings tested.

Crown Copyright © 2008 Published by Elsevier Ltd on behalf of IPEM. All rights reserved.

**Keywords:** ECG; Noise reduction; Adaptive filters; Artifact removal; Biomedical signal analysis; Signal processing

## 1. Introduction

The electrocardiographic (ECG) signal is the electrical representation of the heart's activity. Computerized ECG analysis is widely used as a reliable technique for the diagnosis of cardiovascular diseases, and the ECG signal is the most commonly used biomedical signal in clinical practice [16,20]. However, ambulatory ECG recordings obtained by placing electrodes on the subject's chest are inevitably con-

taminated by several different types of artifacts. Commonly encountered artifacts include baseline wander, power-line interference, physiological signals generated by other organs of the body or induced by muscular contractions related to breathing, and high-frequency random noise.

The removal of artifacts in ECG signals is an essential procedure prior to further diagnostic analysis in many clinical applications, e.g., detection of QRS complexes [10,13], classification of ectopic beats [1,9], analysis of asymptomatic arrhythmia [19], extraction of the fetal ECG signal from the maternal abdominal ECG [11,12], diagnosis of myocardial ischemia [18], diagnosis of atrial fibrillation [27], and ECG data compression [5,28].

\* Corresponding author. Tel.: +86 13910741858.

E-mail addresses: [y.wu@ieee.org](mailto:y.wu@ieee.org) (Y.F. Wu), [ranga@ucalgary.ca](mailto:ranga@ucalgary.ca) (R.M. Rangayyan), [scng@ouhk.edu.hk](mailto:scng@ouhk.edu.hk) (S.-C. Ng).

The extraction of high-resolution ECG signals from recordings contaminated with background noise is an important issue to investigate [4]. The goal for ECG signal enhancement is to separate the valid signal components from the undesired artifacts, so as to present an ECG that facilitates easy and accurate interpretation [2]. Despite the publication of several previous studies in the literature [3,6,14,17,19,23–25], there are still a number of clinical applications that lack effective signal processing tools for efficient and reliable implementation of methods for the filtering and analysis of ECG signals.

In recent years, adaptive filtering has become one of the effective and popular approaches for the processing and analysis of the ECG and other biomedical signals [16]. The fundamental principles of adaptive filtering for noise cancellation were described by Widrow et al. [21]. For stationary signals, the Wiener filter is the optimal linear filtering technique in the minimum mean-squared error (MMSE) sense [8]. Unfortunately, the Wiener filter cannot provide good results when filtering a noisy ECG signal, due to the nonstationary nature of the cardiac signal as well as the noise. The literature contains many alternative adaptive filtering methods that have been used in several practical applications. Xue et al. [26] developed adaptive whitening and matched filters based on artificial neural networks to detect QRS complexes in ECG signals. Thakor and Zhu [19] proposed an adaptive recurrent filter to acquire the impulse response of normal QRS complexes, and then applied it for arrhythmia detection in ambulatory ECG recordings. Hamilton [6] compared adaptive and nonadaptive notch filters for the reduction of power-line interference at 60 Hz. Sameni et al. [17] established a framework of nonlinear Bayesian filtering for ECG noise cancellation.

Although the advantages of adaptive filters for ECG analysis are widely accepted, many such algorithms require detailed study of the features of a given ECG signal, e.g., segmentation of P-QRS-T waves [23], windowing of QRS complexes [17], delineation of artifacts [3], or filter-band reconstruction [2]. These methods consume a significant amount of time for modeling, and are not flexible for application from one patient or condition to another. In this paper, we present a novel unbiased and normalized adaptive noise reduction (UNANR) system for the efficient cancellation of high-frequency random noise in ambulatory ECG recordings.

The remaining parts of this paper are organized as follows. Section 2 provides a description of the adaptive noise-reduction system and the adaptation algorithm of the UNANR model. Section 3 presents the experimental results obtained with 48 noisy ambulatory ECG recordings using the proposed UNANR system, in comparison with those of the prevailing least-mean-square (LMS) filter. Section 4 presents an analysis of the convergence behavior of the UNANR learning rate parameter, and also a discussion on the effects on system performance caused by different values of the learning rate. Section 5 concludes our investigation and

presents potential applications with the proposed UNANR system.

## 2. The unbiased and normalized adaptive noise reduction system

An overview of the proposed UNANR system is provided in Fig. 1. The system contains procedures for signal processing that include a two-stage moving-average filter for the removal of baseline wander, and an infinite impulse response (IIR) comb filter for the removal of periodic power-line interference, which are different in relation to our previous work [24]. A noise generator is placed before the UNANR model in the system, because the focus of the present study is on the reduction of random noise in noisy ambulatory ECG recordings. The details of the aforementioned procedures, together with the adaptation process of the UNANR model, are presented in the following subsections.

### 2.1. Baseline wander removal with a moving-average filter

In the moving-average filter [4], the first- and second-stage averaging window lengths are set to be 1/3 and 2/3 of the length of the input signal in samples, respectively. This filter is used to extract the baseline drift and place the output signal on the isoelectric line of the ECG recording.

### 2.2. Comb filtering with an IIR comb filter

The transfer function of the IIR comb filter with the coefficients specified to 4-decimal-digit word length<sup>1</sup> is

$$H(z) = 0.9502 \frac{1 - z^{-6}}{1 + z^{-1} - 0.9004z^{-6}}. \quad (1)$$

The quality factor ( $Q$  factor) parameter of the IIR comb filter,  $q$ , is defined as the ratio of the frequency to be removed,  $f_0$ , to the filter's bandwidth,  $\text{bw}$ , i.e.,  $q = (2\pi f_0)/\text{bw}$ . The order of the IIR comb filter is determined by the ratio  $f_s/f_0$ , in which  $f_s$  represents the sampling rate of the ECG recordings. For the ECG recordings sampled at 360 Hz, which were studied in our experiments in Section 3, the IIR comb filter with an order of  $360/60 = 6$  and a  $Q$  factor  $q = 30$  provides the frequency response as shown in Fig. 2, which presents a comb filter with rejection bands around 60, 120, and 180 Hz. The zeros and poles of the IIR comb filter are displayed in Fig. 3. Because the order of the IIR comb filter is low, the regions of the zeros and poles appear to be close by, but they do not overlap one another. The impulse response of the IIR comb filter is shown in Fig. 4, from which we can observe

<sup>1</sup> We tested the effect of the coefficients represented using 4, 8, and 16 decimal digits on the IIR comb filter, and found the magnitude and phase responses of the filter to be stable in the finite-word-length implementation.

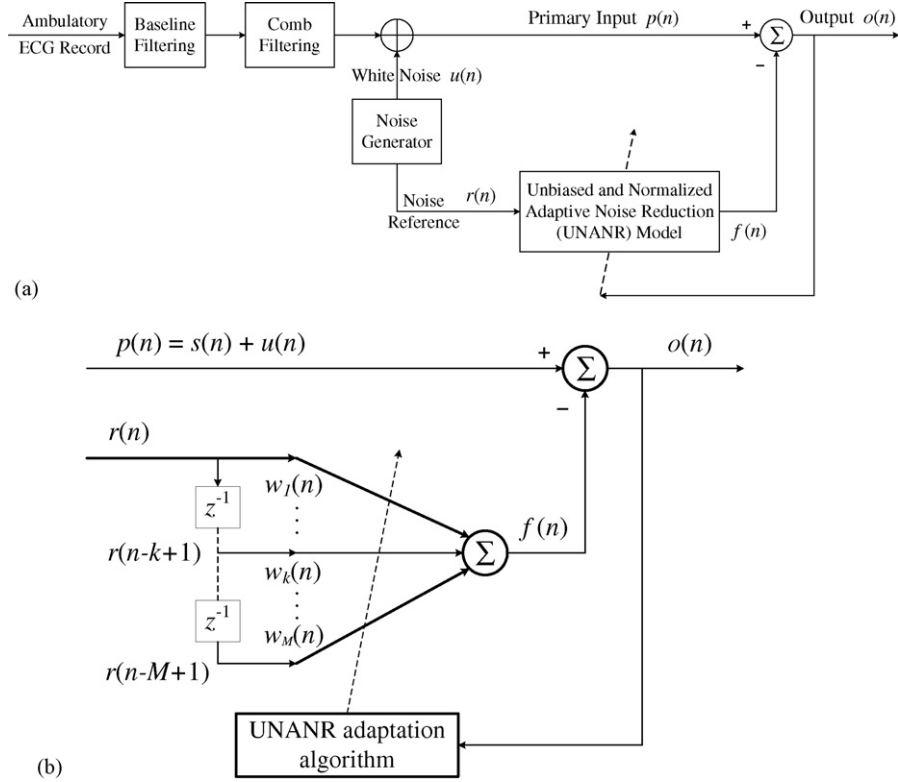


Fig. 1. Overview of the adaptive noise-reduction system. (a) Illustration of the procedures of baseline filtering, comb filtering, noise generator, and proposed UNANR model. (b) Detailed structure of the UNANR model.

that there is no high noise gain introduced by the IIR comb filter.

### 2.3. Additive white noise generator

The noise generator, as depicted in Fig. 1(a), first measures the power of the input signal, and then produces additive white noise with an assigned signal-to-noise ratio (SNR). In the present study, the primary input was contaminated by the additive white noise; the noise generator also provides the noise reference input to the UNANR model. The value of the input SNR was reduced in steps of 2.5 dB from 20 (relatively noise-free) to 5 dB (noisy), because we would like to study the noise-reduction capability of the proposed UNANR model at different levels of the input SNR. The UNANR model gathers information about the noise through its adaptation process, and then provides an estimate of the random noise in ECG signals and the additive white noise, as demonstrated in Section 3, rather than simply subtracting the reference noise.

### 2.4. Unbiased and normalized adaptive noise reduction model

The UNANR model of the system performs the function of adaptive noise estimation. The UNANR model of order  $M$ , as shown in Fig. 1(b), is a transversal, linear, finite impulse response (FIR) filter. The response of the filter  $f(n)$  at each

time instant (sample)  $n$  can be expressed as

$$f(n) = \sum_{m=1}^M w_m(n)r(n - m + 1), \quad (2)$$

where  $w_m(n)$  represents the UNANR coefficients, and  $r(n - m + 1)$  denotes the reference input noise at the present ( $m = 1$ ) and preceding  $m - 1$ , ( $1 < m \leq M$ ), input samples.

In order to provide unit gain at DC, the UNANR coefficients should be normalized such that

$$\sum_{m=1}^M w_m(n) = 1. \quad (3)$$

The adaptation process of the UNANR model is designed to modify the coefficients that get convolved with the reference input in order to estimate the noise present in the given ECG signal. To provide the estimated ECG signal component,  $\hat{s}(n)$ , at the time instant  $n$ , the output of the adaptive noise-reduction system subtracts the response of the UNANR model  $f(n)$  from the primary input  $p(n)$ , i.e.,

$$\hat{s}(n) = o(n) = p(n) - f(n), \quad (4)$$

where the primary input includes the desired ECG component and the additive white noise, i.e.,

$$p(n) = s(n) + u(n). \quad (5)$$

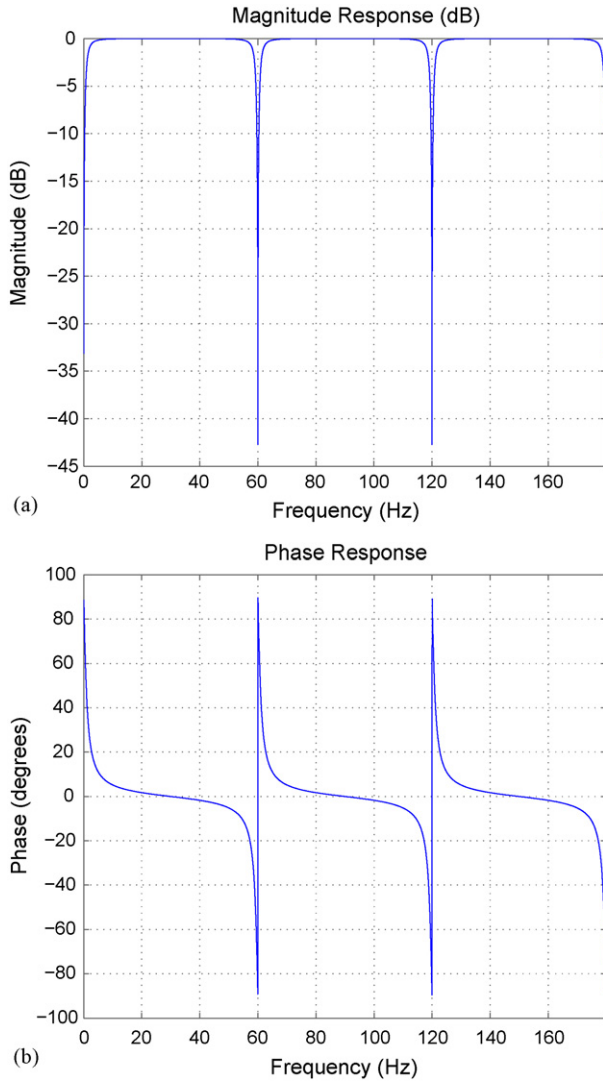


Fig. 2. The frequency response of the 6th-order IIR comb filter with a  $Q$  factor equal to 30, and the input ECG signal sampled at 360 Hz. (a) Magnitude response (dB). (b) Phase response (degrees). The same responses were obtained with the coefficients represented using 4, 8, and 16 decimal digits.

Squaring both sides of (4) yields

$$\begin{aligned}
 \hat{s}^2(n) &= p^2(n) + f^2(n) - 2p(n)f(n) \\
 &= [s(n) + u(n)]^2 + f^2(n) - 2[s(n) + u(n)]f(n) \\
 &= s^2(n) + 2s(n)u(n) + u^2(n) + f^2(n) \\
 &\quad - 2[s(n) + u(n)]f(n). \tag{6}
 \end{aligned}$$

Different from the MMSE criterion, the goal of the UNANR coefficient adaptation process is considered to be the minimization of the instantaneous error  $\epsilon(n)$  between the estimated signal power  $\hat{s}^2(n)$  and the desired signal power  $s^2(n)$ , i.e.,

$$\begin{aligned}
 \epsilon(n) &= \hat{s}^2(n) - s^2(n) = u^2(n) + 2s(n)u(n) + f^2(n) \\
 &\quad - 2[s(n) + u(n)]f(n). \tag{7}
 \end{aligned}$$

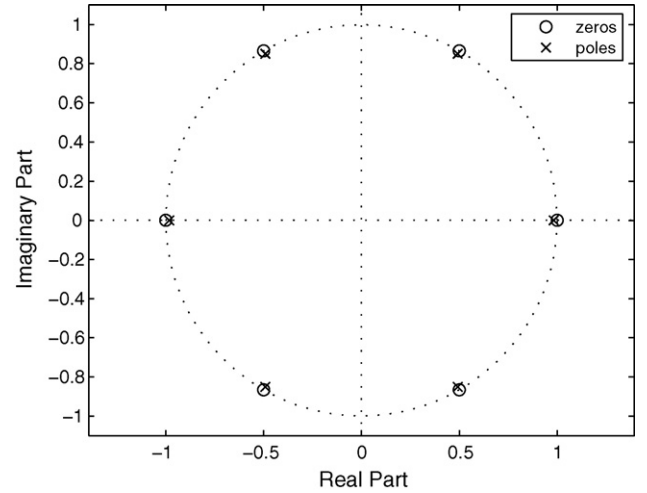


Fig. 3. The zeros and poles of the 6th-order IIR comb filter, with the input ECG signal sampled at 360 Hz.

Such a goal can be achieved by optimizing the UNANR coefficients according to the steepest-descent algorithm [7]. The process of convergence in the multidimensional coefficient space follows a deterministic search path provided by the negative gradient direction as

$$\begin{aligned}
 -\nabla_{w_k} \epsilon(n) &= -\frac{\partial f^2(n)}{\partial w_k} + 2 \frac{\partial [s(n) + u(n)]f(n)}{\partial w_k} \\
 &= -2r(n-k+1) \sum_{m=1}^M w_m(n)r(n-m+1) \\
 &\quad - 2p(n)r(n-k+1) = -2r(n-k+1) \\
 &\quad \times \left[ \sum_{m=1}^M w_m(n)r(n-m+1) - p(n) \right]. \tag{8}
 \end{aligned}$$

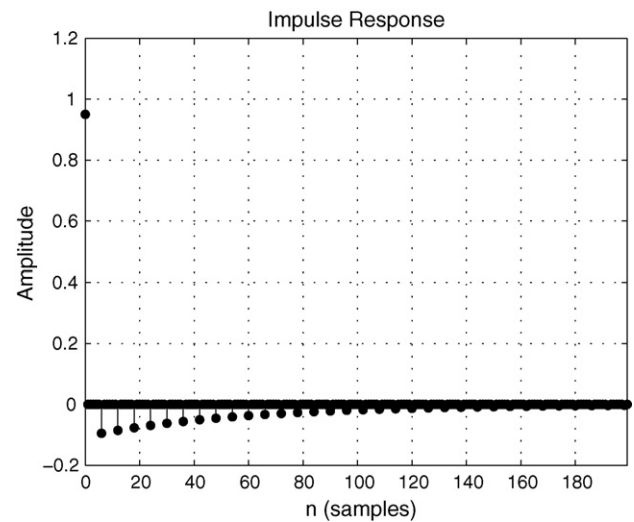


Fig. 4. The impulse response of the 6th-order IIR comb filter.

By substituting (3) and (8) into the standard steepest-descent algorithm [7], we may derive the UNANR adaptation rule as

$$\begin{aligned} w_k(n+1) &= w_k(n) - \eta \nabla_{w_k} \epsilon(n) = w_k(n) - 2\eta r(n-k+1) \\ &\quad \times \left[ \sum_{m=1}^M w_m(n) r(n-m+1) - p(n) \right] \\ &= w_k(n) + 2\eta r(n-k+1) \sum_{m=1}^M w_m(n) [p(n) \\ &\quad - r(n-m+1)], \end{aligned} \quad (9)$$

where  $\eta$  ( $\eta > 0$ ) represents the learning rate that indicates the search magnitude in the negative gradient direction.

Before the UNANR model provides its response  $f(n+1)$  referring to (2), at each time instant  $n+1$ , the estimated coefficients  $\hat{w}_k(n+1)$  should be normalized so as to meet the requirement of (3). The UNANR coefficient normalization formulation is given by

$$\hat{w}_k(n+1) = \frac{w_k(n+1)}{\sum_{k=1}^M w_k(n+1)}. \quad (10)$$

Table 1  
Summary of the UNANR coefficient initialization and adaptation procedures

Variables and parameters	
$n$ :	time instant, a unit of which equals to $1/f_s$
$r(n)$ :	present noise reference input sample
$r(n-m+1)$ :	preceding $m-1$ , ( $1 < m \leq M$ ), noise reference input samples
$p(n)$ :	present noise-contaminated primary input sample
$\eta$ :	learning-rate parameter, a positive constant
$w_k(n)$ :	instantaneous value of the $k$ th coefficient during the adaptation process
$\hat{w}_k(n+1)$ :	estimated value of the $k$ th normalized coefficient for time instant $n+1$
$f(n)$ :	response of the UNANR model at time instant (sample) $n$
Procedure	
1. <i>Initialization.</i>	Set the coefficients to uniformly distributed random values with zero mean and unit variance. Normalize the coefficients to have unit sum
2. <i>Activation.</i>	At time instant $n$ , activate the UNANR model with noise reference $r(n)$ and estimated values of the coefficients $\hat{w}_k(n)$
	$f(n) = \sum_{m=1}^M \hat{w}_m(n) r(n-m+1)$
3. <i>Adaptation of coefficients.</i>	Update the coefficients for the next time instant $n+1$
	$w_k(n+1) = w_k(n) + 2\eta r(n-k+1) \sum_{m=1}^M w_m(n) [p(n) - r(n-m+1)]$
	$\hat{w}_k(n+1) = \frac{w_k(n+1)}{\sum_{k=1}^M w_k(n+1)}$
4. <i>Continuation.</i>	Increment time instant $n$ by one and go back to Step 2

The procedures of initialization and adaptation of the UNANR coefficients are summarized in Table 1. The UNANR adaptation procedure does not include the computation of estimating the signal power error  $\epsilon(n)$ , because the gradient descent of  $\epsilon(n)$  during the convergence process can be obtained with respect to the primary input and the time-lagged reference noise inputs, referring to (8). In real-time implementation, the UNANR model can provide its response with a delay of only  $(M-1)$  samples, or  $(M-1)/f_s$  seconds; however, the characteristic of updating coefficients directly with regard to the primary input and the time-lagged noise reference inputs enables the UNANR model to perform faster digital signal processing (DSP) in applications of ambulatory ECG monitoring, in comparison with the other popular methods, such as the LMS filter. Moreover, the estimation of noise components ensures that the performance of the proposed UNANR model is independent of the analysis of ECG features, which obviates the consumption of a significant amount of time for signal or noise modeling, as required by the conventional approaches.

### 3. Experiments and results

We used the benchmark MIT-BIH arrhythmia database [15] to evaluate the performance of the proposed adaptive noise-reduction system. The database consists of 48 half-hour excerpts of two-channel ambulatory ECG recordings, which were obtained from 47 subjects, including 25 men aged 32–89 years, and 22 women aged 23–89 years (Tape Nos. 201 and 202 records are from the same male subject). The ECG signal we studied is the modified limb lead II (MLII) in the first channel of the recording data, each of which contains 21,600 samples digitized at 360 Hz with 11-bit resolution over a 10 mV range.

All of the ECG filtering experiments were run in MATLAB<sup>®</sup> v. 7.0 (The MathWorks, Inc.). The coefficients of the IIR comb filter were obtained with the *ircomb* function of the Filter Design Toolbox v. 3.2, and the additive white noise generator was implemented with the *awgn* function of the Communications Toolbox v. 3.1. Both of the toolboxes are included in MATLAB<sup>®</sup> v. 7.0. All of the analyses were performed on a DELL<sup>®</sup> laptop computer with an Intel<sup>®</sup> Pentium<sup>®</sup> M processor of 1.86 GHz speed, and with 1.5 GB RAM, under Microsoft<sup>®</sup> Windows XP<sup>®</sup> Professional (32-bit system).

Fig. 5 gives a sample result of baseline filtering with the first 10 s of the ECG Tape No. 101 record. It can be observed that the baseline wander has been effectively removed in the filtered signal in Fig. 5(c), by subtracting from the original input the drift extracted by the two-stage moving-average filter, shown in Fig. 5(b).

The effect of comb filtering with the IIR comb filter is shown in Fig. 6. The input to the IIR comb filter is the baseline-wander-free signal with the power spectrum, as shown in Fig. 6(a). It is clear from Fig. 6(b) that the

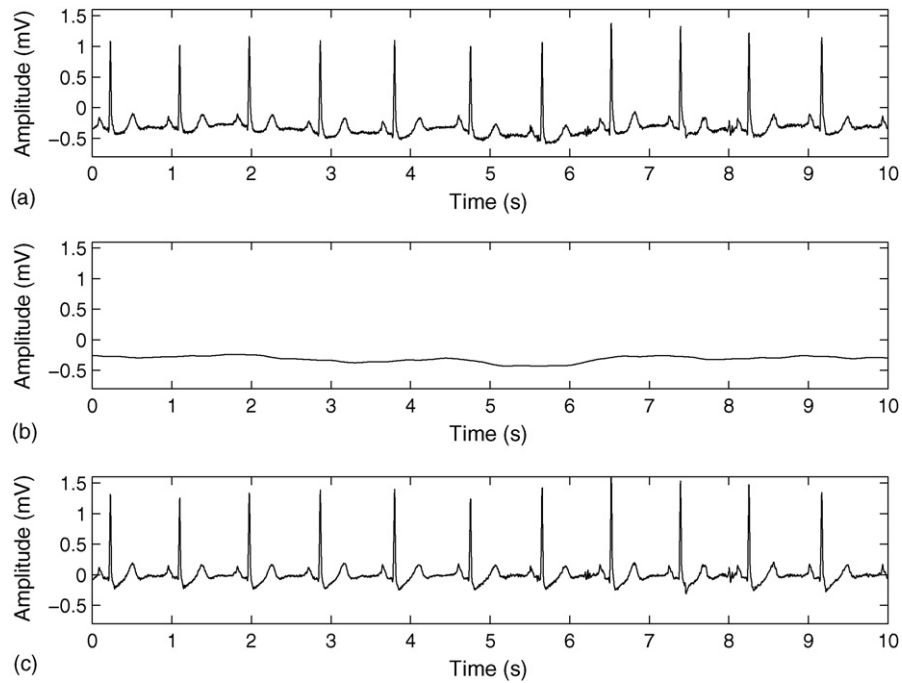


Fig. 5. Illustration of baseline filtering with the first 10 s of the ECG Tape No. 101 record. (a) Original ECG record. (b) Baseline wander extracted by the two-stage moving-average filter. (c) The filtered signal.

power-line interference at 60, 120, and 180 Hz has been eliminated. For the input ECG signal sampled at 360 Hz, the quality factor  $q$  of the IIR comb filter was set to be 30, which rejects a range of frequencies that is narrow in comparison with the center frequencies at 60 Hz and its harmonics. This ensures that there is no significant

distortion of the ECG waveform introduced by the comb filter.

For comparison of adaptive noise-reduction performance, we also implemented the popular LMS adaptive filter [8], which was used in place of the UNANR model in the system. The coefficient order and learning rate of the LMS filter

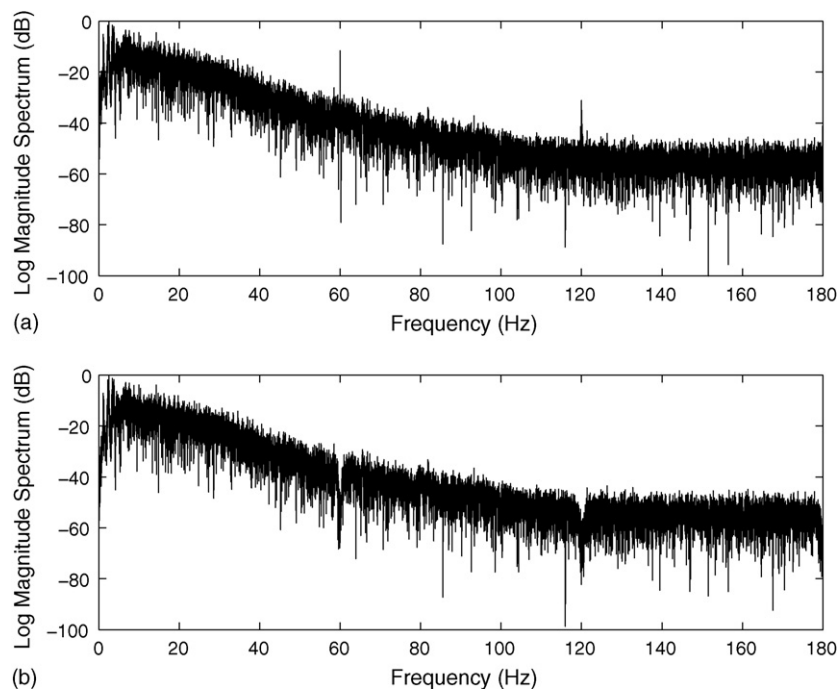


Fig. 6. Illustration of the effect of the 6th-order IIR comb filter in the frequency domain. (a) Power spectrum of the ECG Tape No. 101 record after baseline filtering. (b) Power spectrum of the output of the IIR comb filter.

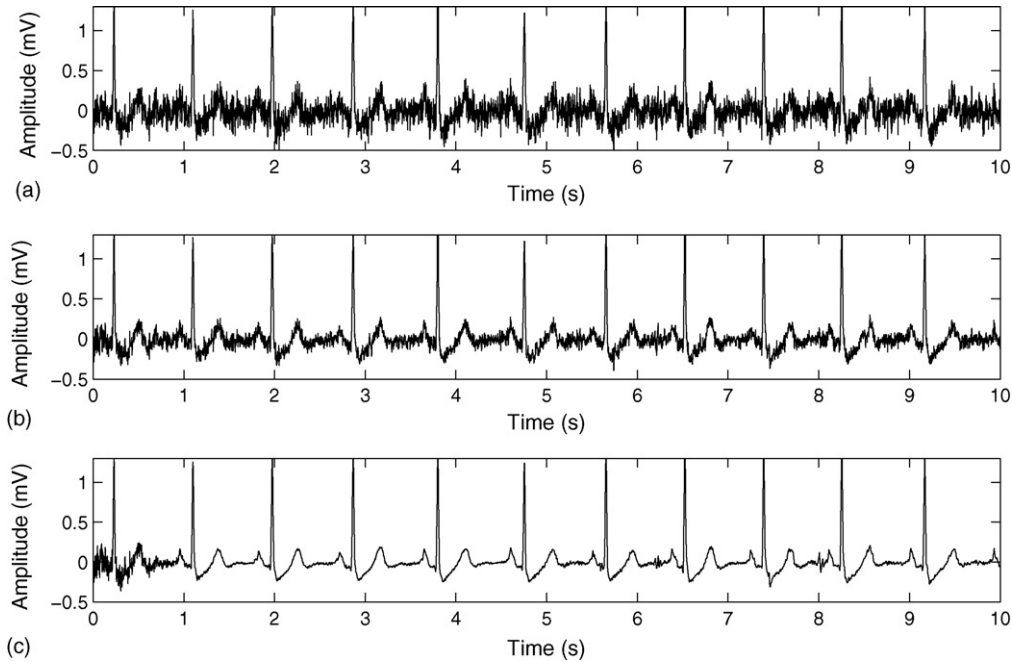


Fig. 7. Illustration of the effect of the adaptive noise-reduction system with the first 10 s of the ECG Tape No. 101 record. (a) ECG signal (after baseline and comb filtering) contaminated by white noise (input SNR: 5 dB). (b) Adaptive noise-reduction system output using the LMS filter. (c) Adaptive noise-reduction system output using the UNANR model.

and the UNANR model were set to be the same,<sup>2</sup> as  $M = 10$  and  $\eta = 0.5$ . The results of the system's performance are illustrated in Fig. 7. The primary input to the system, shown in Fig. 7(a), was a mixture of white noise with the SNR of 5 dB and the ECG signal after baseline and comb filtering. The LMS filter does not effectively achieve noise cancellation, because the system's output still remains noisy. In addition, the outlines of the P and T waves in Fig. 7(b) are not distinct, and such a result is not suitable for clinical applications. Considering the results of the UNANR system in Fig. 7(c), we find that the noise-reduction performance of the UNANR model is better: The components of random noise have become weaker, and the ECG features are prominently visible from the second cardiac beat onwards.

For quantitative evaluation, we define the SNR improvement achieved by the adaptive noise-reduction system to be the value of the system output SNR (in dB) minus the input SNR (in dB). The mean and standard deviation (S.D.) of the SNR improvement versus different levels of the input SNR, obtained from the 48 ECG recordings tested, are plotted in Fig. 8. The primary input to the system varies being from relatively noise-free (input SNR: 20 dB) to being noisy (input

SNR: 5 dB). It can be observed that the SNR improvement curve with regard to the LMS filter does not increase much, but remains around the level of 5 dB. The reason for this could be that the noise-reduction capability of the system with the LMS filter does not change much with the nature of the primary input, and that the system performance is only determined by the learning rate parameter of the LMS filter. Regarding the UNANR model, on the other hand, the system's SNR improvement curve increases from 10.22 to

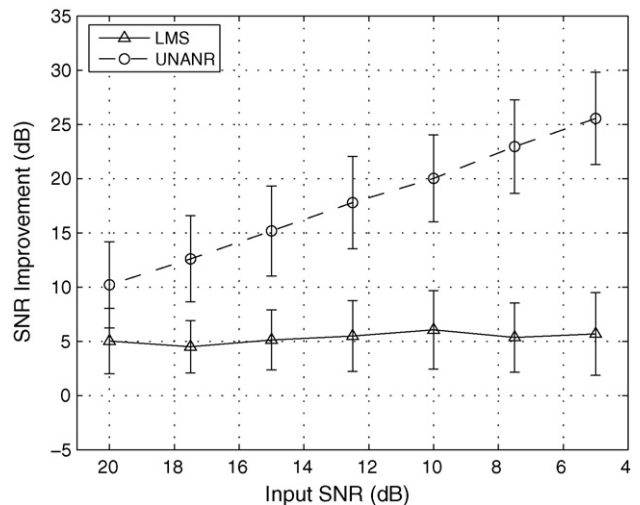


Fig. 8. Plot of the mean and standard deviation (S.D.) of the system's SNR improvement with respect to the LMS filter (triangle) and the UNANR model (circle) versus different levels of the input SNR.

<sup>2</sup> The convergence ranges of the learning rates for the LMS filter and the UNANR model are different. The coefficients of the LMS filter frequently did not converge when  $\eta$  was larger than 1.0 with most of the signals tested, which represents degradation of the system output SNR. For this reason, we fixed  $\eta$  to be 0.5 in the filters for comparison. Further study on the convergence behavior of the UNANR learning rate is described in Section 4.

Table 2  
SNR improvement using the LMS filter and the UNANR model, with different levels of the input SNR

Input SNR (dB)	SNR improvement using the LMS filter		SNR improvement using the UNANR model	
	Mean (dB)	S.D.	Mean (dB)	S.D.
5.0	5.69	3.80	25.56	4.26
7.5	5.36	3.19	22.97	4.31
10.0	6.07	3.62	20.03	4.00
12.5	5.50	3.27	17.80	4.26
15.0	5.13	2.76	15.19	4.15
17.5	4.51	2.41	12.61	3.98
20.0	5.03	3.03	10.22	3.98

25.56 dB, as listed in Table 2, when the input becomes more and more heavily contaminated by white noise. It can be inferred that the proposed UNANR system, when its learning rate parameter is fixed, is able to behave adaptively with variation of the white noise present in the primary input. In the following section, we investigate the convergence behavior of the UNANR learning rate, together with the effects on system performance caused by different values of  $\eta$ .

#### 4. Study on convergence of the UNANR learning rate

Referring to (9), we can deduce that the convergence process of the UNANR adaptation algorithm is influenced by the value assigned to the learning rate parameter  $\eta$  and the statistical characteristics of the  $M$ -element reference input vector  $\mathbf{r}(n) = [r(n), r(n-1), \dots, r(n-M+1)]^T$ . According to Widrow's independence theory [22], the UNANR adaptation algorithm is convergent in the mean-squared sense provided that  $\eta$  satisfies the condition [8]:

$$0 < \eta < \frac{2}{\lambda_{\max}}, \quad (11)$$

where  $\lambda_{\max}$  is the largest eigenvalue of the correlation matrix  $\mathbf{C}_r$  of the input signal, i.e.,

$$\mathbf{C}_r = E[\mathbf{r}(n)\mathbf{r}^T(n)]. \quad (12)$$

For the inherently nonstationary ECG signal, the Wiener solution of the UNANR coefficients is difficult to obtain, because there is no prior knowledge of  $\lambda_{\max}$  available. To overcome this difficulty, the trace of  $\mathbf{C}_r$  may be taken as a conservative estimate of  $\lambda_{\max}$ . Because the correlation matrix  $\mathbf{C}_r$  is a square matrix, its trace is the sum of the diagonal elements, each of which equals the mean-squared value of the corresponding input signal. The condition for convergence of the UNANR adaptation algorithm can then be formulated as

$$0 < \eta < \frac{2}{M}. \quad (13)$$

The effects on system performance caused by a particular UNANR learning rate can also be noted from the corresponding SNR improvement of the system. Fig. 9 provides an

illustration of the system's SNR improvement versus different values of  $\eta$ . For the ECG Tape No. 101 record studied, the four empirical curves of the system's SNR improvement, with various levels of the input SNR, consistently ascend to reach the corresponding maximum values, and then begin to descend when the learning rate is larger than 6.0 in most cases. We also see that the slope of the system's SNR improvement curve versus the learning rate increases with larger input SNR. For example, the SNR improvement curve with the input SNR of 5 dB has a 12.79 dB increment from  $\eta = 0.5$  to 6.5, whereas the corresponding curve with input SNR of 20 dB only grows with an 8.18 dB increment. Besides achieving better SNR improvement, the proper value of the learning rate also provides faster convergence during adaptive filtering. Under the same condition of the input SNR (5 dB, for example), we note from Fig. 10(c) that the UNANR system with  $\eta = 6.0$  performs effectively within a single cardiac cycle, whereas the system with the learning rate of 1.0 can only provide a noise-free ECG signal from the third cardiac beat onwards, as shown in Fig. 10(b).

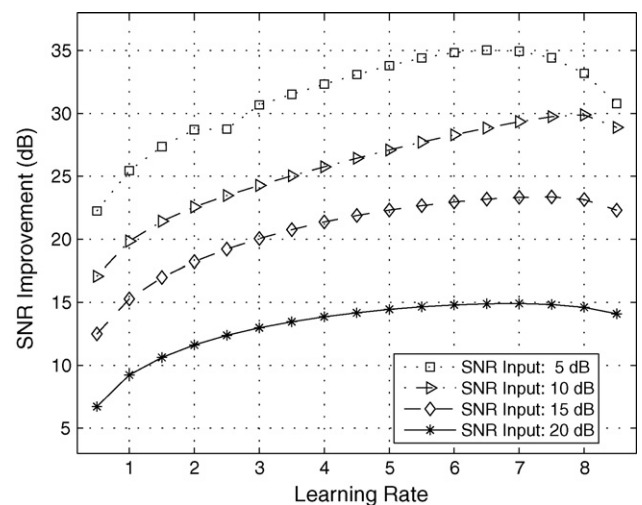


Fig. 9. The system's SNR improvement versus a range of the learning rates of the UNANR model. The input signal is the ECG Tape No. 101 record contaminated by white noise with different levels of the input SNR.



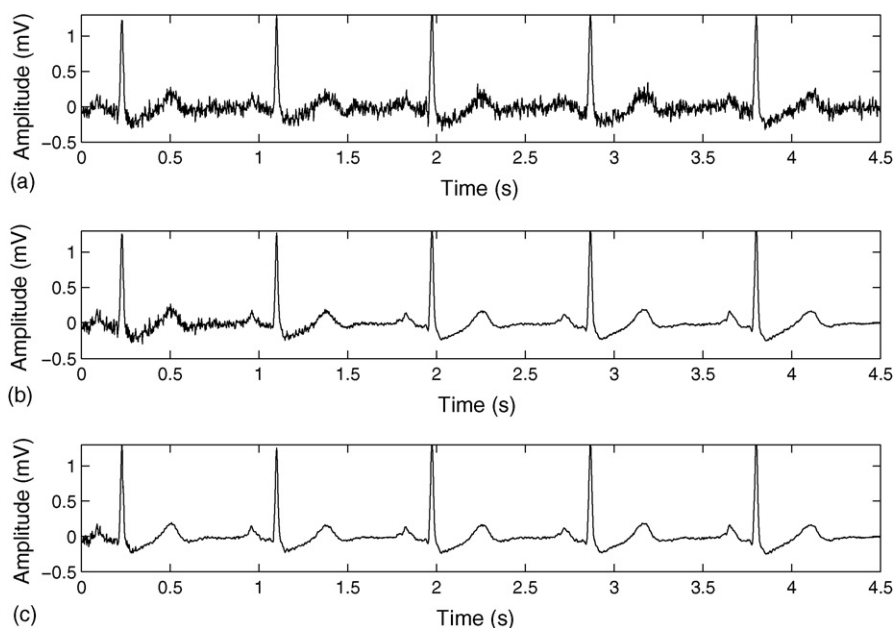


Fig. 10. Illustration of the UNANR system output with different values of the learning rate. (a) The first 4.5 s of the ECG Tape No. 101 signal (after baseline and comb filtering) contaminated by white noise (input SNR: 5 dB). (b) The UNANR system output with the learning rate  $\eta = 1.0$ . (c) The UNANR system output with the learning rate  $\eta = 6.0$ .

## 5. Conclusion

The results obtained in our experiments demonstrate the tangible advantages of the proposed UNANR system for adaptive noise reduction in ECG signals. The noise filtering provided by the UNANR model is more effective than that resulting from the popular LMS filter, especially with the high level of noise present in the ECG records tested. In addition, the adaptation process of the UNANR model is also simple to implement, without the need to identify the features of the ECG signals, such as detection of QRS complexes. Once the proper value of the learning rate parameter is determined, the UNANR system can provide the output of noise-free ECG signal rapidly. For clinical application in long-term ECG monitoring, conventional techniques require a high complexity for the computation of the system's parameters, and demand much effort from the user on signal modeling. The proposed UNANR system can overcome such drawbacks, and is well-suited for ECG monitoring in practical applications.

## Acknowledgments

This work was supported in part by the National Science Foundation of China under Grant No. 60575034; the Doctoral Program Foundation of the Ministry of Education of China under Grant No. 20060013007; and the 2005 Innovation Research Funds from the Graduate School, Beijing University of Posts and Telecommunications. Y.F. Wu received the 2007 "Visitorship for Scholar in Mainland of China" grant

sponsored by the Croucher Foundation in Hong Kong. R.M. Rangayyan has been supported by the University of Calgary in the form of a "University Professorship."

## References

- [1] Afonso VX, Tompkins WJ, Nguyen TQ, Luo S. ECG beat detection using filter banks. *IEEE Trans Biomed Eng* 1999;46(2):192–202.
- [2] Afonso VX, Tompkins WJ, Nguyen TQ, Michler K, Luo S. Comparing stress ECG enhancement algorithms. *IEEE Eng Med Biol Mag* 1996;15(3):37–44.
- [3] Blanco-Velasco M, Weng B, Barner KE. A new ECG enhancement algorithm for stress ECG tests. In: *Proceedings of the 2006 computers in cardiology conference (CINC'06)*. 2006. p. 917–20.
- [4] Clifford GD, Azuaje F, McSharry P. *Advanced methods and tools for ECG data analysis*. Norwood, MA: Artech House; 2006.
- [5] Hamilton DJ, Thomson DC, Sandham WA. ANN compression of morphologically similar ECG complexes. *Med Biol Eng Comput* 1995;33(6):841–3.
- [6] Hamilton PS. A comparison of adaptive and nonadaptive filters for reduction of power line interference in the ECG. *IEEE Trans Biomed Eng* 1996;43(1):105–9.
- [7] Haykin S. *Neural networks: a comprehensive foundation*. 2nd ed Englewood Cliffs, NJ: Prentice Hall PTR; 1998.
- [8] Haykin S. *Adaptive filter theory*. 4th ed Englewood Cliffs, NJ: Prentice Hall PTR; 2002.
- [9] Hu YH, Palreddy S, Tompkins WJ. A patient-adaptable ECG beat classifier using a mixture of experts approach. *IEEE Trans Biomed Eng* 1997;44(9):891–900.
- [10] Hu YH, Tompkins WJ, Urrusti JL, Afonso VX. Applications of artificial neural networks for ECG signal detection and classification. *J Electrocardiol* 1993;26(Suppl.):66–73.
- [11] Kanjilal PP, Palit S, Saha G. Fetal ECG extraction from single-channel maternal ECG using singular value decomposition. *IEEE Trans Biomed Eng* 1997;44(1):51–9.

- [12] Khamene A, Negahdaripour S. A new method for the extraction of fetal ECG from the composite abdominal signal. *IEEE Trans Biomed Eng* 2000;47(4):507–16.
- [13] Meyer C, Gavela JF, Harris M. Combining algorithms in automatic detection of QRS complexes in ECG signals. *IEEE Trans Inf Technol in Biomed* 2006;10(3):468–75.
- [14] Mneimneh MA, Yaz EE, Johnson MT, Povinelli RJ. An adaptive Kalman filter for removing baseline wandering in ECG signals. In: *Proceedings of the 2006 computers in cardiology conference (CINC'06)*. 2006. p. 253–6.
- [15] Moody GB, Mark RG, Goldberger AL. Physionet: a web-based resource for the study of physiologic signals. *IEEE Eng Med Biol Mag* 2001;20(3):70–5.
- [16] Rangayyan RM. *Biomedical signal analysis: a case-study approach*. New York, NY: IEEE and Wiley; 2002.
- [17] Sameni R, Shamsollahi MB, Jutten C, Clifford GD. A nonlinear Bayesian filtering framework for ECG denoising. *IEEE Trans Biomed Eng* 2007;54(12):2172–85.
- [18] Silipo R, Marchesi C. Artificial neural networks for automatic ECG analysis. *IEEE Trans Signal Process* 1998;46(5):1417–25.
- [19] Thakor NV, Zhu YS. Applications of adaptive filtering to ECG analysis: noise cancellation and arrhythmia detection. *IEEE Trans Biomed Eng* 1991;38(8):785–94.
- [20] Tompkins WJ. *Biomedical digital signal processing: C language examples and laboratory experiments for the IBM PC*. Englewood Cliffs, NJ: Prentice Hall PTR; 1993.
- [21] Widrow B, Glover JR, McCool JM, Kaunitz J, Williams CS, Hearn RH, et al. Adaptive noise cancelling: principles and applications. *Proc IEEE* 1975;63(12):1692–716.
- [22] Widrow B, McCool JM, Larimore MG, Johnson Jr CR. Stationary and nonstationary learning characteristics of the LMS adaptive filter. *Proc IEEE* 1976;64(8):1151–62.
- [23] Wu YF, Rangayyan RM. An unbiased linear artificial neural network with normalized adaptive coefficients for filtering noisy ECG signals. In: *Proceedings of the 20th Canadian conference on electrical and computer engineering (CCECE'07)*. 2007. p. 868–71.
- [24] Wu YF, Rangayyan RM, Ng SC. Cancellation of artifacts in ECG signals using a normalized adaptive neural filter. In: *Proceedings of the 29th annual international conference IEEE engineering in medicine and biology society (EMBC'07)*. 2007. p. 2552–5.
- [25] Wu YF, Rangayyan RM, Wu Y, Ng SC. Filtering of noise in electrocardiographic signals using an unbiased and normalized adaptive artifact cancellation system. In: *Proceedings of the 6th international symposium on noninvasive functional source imaging of the brain and heart (NFSI'07)*. China: Hangzhou; 2007. p. 173–6.
- [26] Xue Q, Hu YH, Tompkins WJ. Neural-network-based adaptive matched filtering for QRS detection. *IEEE Trans Biomed Eng* 1992;39(4):317–29.
- [27] Yang TF, Devine B, Macfarlane PW. Artificial neural networks for the diagnosis of atrial fibrillation. *Med Biol Eng Comput* 1994;32(6):615–9.
- [28] Zigel Y, Cohen A, Katz A. ECG signal compression using analysis by synthesis coding. *IEEE Trans Biomed Eng* 2000;47(10):1308–16.